

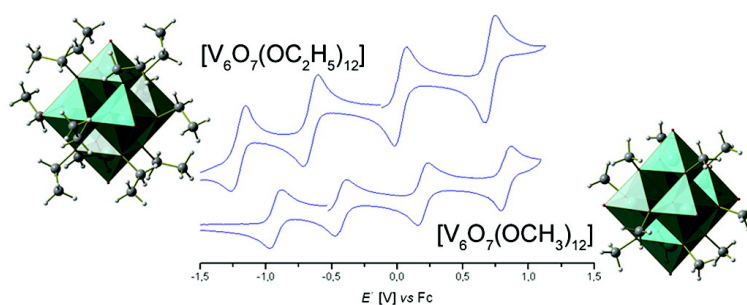
Article

# Neutral and Cationic V/V Mixed-Valence Alkoxo-polyoxovanadium Clusters $[VO(OR)]$ ( $R = -CH_2, -CH_3$ ): Structural, Cyclovoltammetric and IR-Spectroscopic Investigations on Mixed Valency in a Hexanuclear Core

Charles Daniel, and Hans Hartl

*J. Am. Chem. Soc.*, **2005**, 127 (40), 13978-13987 • DOI: 10.1021/ja052902b • Publication Date (Web): 15 September 2005

Downloaded from <http://pubs.acs.org> on March 25, 2009



## More About This Article

Additional resources and features associated with this article are available within the HTML version:

- Supporting Information
- Links to the 6 articles that cite this article, as of the time of this article download
- Access to high resolution figures
- Links to articles and content related to this article
- Copyright permission to reproduce figures and/or text from this article

[View the Full Text HTML](#)



ACS Publications  
 High quality. High impact.

## Neutral and Cationic V<sup>IV</sup>/V<sup>V</sup> Mixed-Valence Alkoxo-polyoxovanadium Clusters [V<sub>6</sub>O<sub>7</sub>(OR)<sub>12</sub>]<sup>n+</sup> (R = -CH<sub>3</sub>, -C<sub>2</sub>H<sub>5</sub>): Structural, Cyclovoltammetric and IR-Spectroscopic Investigations on Mixed Valency in a Hexanuclear Core

Charles Daniel\* and Hans Hartl

Contribution from the Institut für Chemie/Anorganische und Analytische Chemie, Freie Universität Berlin, Fabekstrasse 34-36, 14195 Berlin, Germany

Received May 3, 2005; E-mail: charles.daniel@web.de

**Abstract:** The alkoxo-polyoxovanadium clusters [V<sub>6</sub>O<sub>7</sub>(OR)<sub>12</sub>] (R = -CH<sub>3</sub>, -C<sub>2</sub>H<sub>5</sub>) are fully alkylated polyoxometalate derivatives comprising a hexavanadate core with the vanadium ions organized in an octahedral fashion, a classic isopolyoxometalate structure (Lindqvist) which as an entity is not known for vanadium. The clusters are highly redox-active compounds, displaying a large number of thermodynamically stable redox isomers of which the chemical syntheses and structural characterization of the neutral and cationic V<sup>IV</sup>/V<sup>V</sup> mixed-valence species [V<sup>IV</sup><sub>(4-n)</sub>V<sup>V</sup><sub>(2+n)</sub>O<sub>7</sub>(OR)<sub>12</sub>]<sup>n+</sup>[SbCl<sub>6</sub>]<sub>n</sub> (R = -CH<sub>3</sub>, n = 0, 1; R = -C<sub>2</sub>H<sub>5</sub>, n = 0, 1, 2) are presented here. Neutral and positively charged clusters remain exceptional in the field of polyoxometalate chemistry. Results obtained from cyclic voltammetry, infrared spectroscopy, and from valence sum calculations conducted on X-ray structural data classify these clusters as class II mixed-valence compounds. Their highly symmetrical molecular structures make them particularly interesting as model compounds for the investigation of intervalence charge transfer and electron delocalization in the hexanuclear core. Furthermore, the large number of isostructural redox isomers affords a high variability in d-electron content. Accordingly, a dependency could clearly be established between the extent of electron delocalization and the V<sup>IV</sup>/V<sup>V</sup> ratio in a cluster species. A further interesting observation concerns the neutral ethoxo compound [V<sup>IV</sup><sub>4</sub>V<sup>V</sup><sub>2</sub>O<sub>7</sub>(OC<sub>2</sub>H<sub>5</sub>)<sub>12</sub>] (**3**) which exhibits a crystallographic phase transition accompanied by the conversion from a structure at 173 K with fully localized valencies to a room-temperature modification displaying complete d-electron delocalization.

### Introduction

The early transition metals (V, Nb, Ta, Mo, W) play an important role in metal oxide chemistry due to their ability to form polyoxometalates. By virtue of both their charge-to-radius ratio and their ability to engage in metal–oxygen dπ–pπ interactions, these metals in their highest oxidation states (d<sup>0</sup>, d<sup>1</sup>) are able to form defined polynuclear anionic species in solution, thus allowing an exclusive chemistry in a field which for the rest is more or less banned to the solid state. Research on polyoxometalates has brought forth a wealth of compounds and structures, equally incorporating a variety of metals and nonmetals as heteroatoms.<sup>1</sup> In addition to their intriguing structural diversity as well as interesting magnetic<sup>2</sup> and electrochemical properties,<sup>3</sup> they have revealed a multitude of applications in various domains such as catalysis, medicine, and materials science.<sup>1b,4</sup>

In the past 30 years, extensive use of organic and organo-metallic components in the synthesis of polyoxometalate deriva-

tives gave rise to a surge of new compounds and structures.<sup>5</sup> This progress, preceded by the introduction of organic counterions such as tetra-*n*-butylammonium which marked the beginning of polyoxometalate chemistry in organic solvents,<sup>6</sup> expanded their reach to practically all relevant fields of chemistry.

Alkoxo-polyoxometalates, i.e., polyoxometalates incorporating alkoxo ligands, represent the largest subclass of polyoxometalate derivatives.<sup>7</sup> The introduction of oxygen donor-ligands in polyoxometalates allows charge compensation via formal substitution of peripheral, generally bridging oxo ligands, thus stabilizing otherwise unstable polyoxometalate architectures.<sup>5a</sup> Among other novel structures, this made it possible to synthesize alkoxo-polyoxometalates containing the hexavanadate core {V<sub>6</sub>O<sub>19</sub>},<sup>5a,8</sup> one of the classical polyoxometalate structures

(1) (a) Pope, M. T. *Heteropoly and Isopoly Oxometalates*; Springer: Berlin, 1983. (b) Pope, M. T.; Müller, A. *Angew. Chem., Int. Ed. Engl.* **1991**, *30*, 34–48. (c) Baker, L. C.; Glick, D. C. *Chem. Rev.* **1998**, *98*, 3–50. (d) Pope, M. T. In *Comprehensive Coordination Chemistry II*; McCleverty, J. A., Meyer, T. J., Eds.; Elsevier: Oxford 2004; Vol. 4, 635–678. (2) Müller, A.; Peters, F.; Pope, M. T.; Gatteschi, D. *Chem. Rev.* **1998**, *1*, 239–272. (3) Sadakane, M.; Steckhan, E. *Chem. Rev.* **1998**, *98*, 219–238.

(4) (a) Kozevnikov, I. *Catalysis by Polyoxometalates*; John Wiley & Sons: Chichester, 2002. (b) Yamase, T., Pope, M. T., Eds.; *Polyoxometalate Chemistry for Nano-Composite Design*; Kluwer/Plenum: New York, 2002. (c) Pope, M. T., Müller, A., Eds.; *Polyoxometalates: From Platonic Solids to Anti-Retroviral Activity*; Kluwer: Dordrecht, 1994. (5) (a) Gouzerh, P.; Proust, A. *Chem. Rev.* **1998**, *98*, 77–111. (b) Khan, M. I.; Zubieta, J. *Prog. Inorg. Chem.* **1995**, *43*, 1–149. (6) Fuchs, J. *Z. Naturforsch.* **1973**, *28b*, 389. (7) Bradley, D. C.; Mehrotra, R. C.; Rothwell, I. P.; Singh, A. *Alkoxo and Aryloxo Derivatives of Metals*; Academic Press: London, 2001. (8) Piepenbrink, M.; Triller, M. U.; Gorman, N. H. J.; Krebs, B. *Angew. Chem., Int. Ed.* **2002**, *41*, 2523–2525.

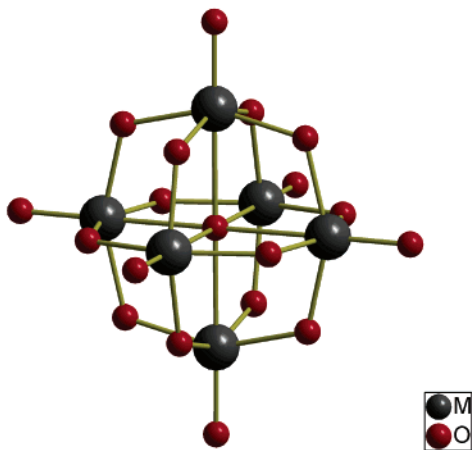


Figure 1. The Lindqvist structure.

formed by Mo, W, Nb and Ta, which is not known for vanadium, probably due to the small ionic radius of  $V^V$  in combination with the high charge of the theoretical  $[V_6O_{19}]^{8-}$  anion. Especially Zubieta et al. were successful in synthesizing a variety of such compounds incorporating trisalkoxo  $\mu$ -bridging moieties.<sup>5b</sup> Our interest of research concerns related alkoxo-polyoxometal species of the general composition  $[V^{IV}_n V^{V}_{6-n} O_7(OR)_{12}]^{(4-n)-}$ . These cluster compounds are formally derived from the Lindqvist structure<sup>9</sup>  $[M_6O_{19}]^{n-}$  (Figure 1) by substitution of all twelve  $\mu$ -bridging oxo ligands with monodentate alkoxo ligands. Compounds of this type have been synthesized with methoxo ligands.<sup>10</sup>

In this article we describe the synthesis and crystal structures of the neutral alkoxo-polyoxovanadium clusters  $[V^{IV}_4 V^{V}_2 O_7(OR)_{12}]$  ( $R = -CH_3, -C_2H_5$ ), as well as three cationic derivatives of the general composition  $[V^{IV}_{(4-n)} V^{V}_{(2+n)} O_7(OR)_{12}]^{n+}$  ( $R = -CH_3, n = 1$ ;  $R = -C_2H_5, n = 1, 2$ ) obtained by chemical oxidation of the neutral compounds. Neutral and cationic species are a rare instance among polyoxometalates<sup>11</sup> and their derivatives,<sup>12</sup> the positively charged clusters reported herein being to our knowledge the first cationic alkoxo-polyoxometal clusters known to date.<sup>13</sup> Although we have previously reported the monocationic methoxo-polyoxovanadium cluster  $[V^{IV}_3 V^{V}_3 O_7(OCH_3)_{12}]^+$  in polyhalide salts,<sup>10</sup> the hexachloroantimonate salt reported here offers the advantage of being easily synthesized and of containing a counterion which is, to a large extent, chemically inert. Furthermore, for sake of adequate comparison of the compounds' crystal structures and properties, the salts presented here all contain hexachloroantimonate as the anion.

Among the compounds we have synthesized, the alkoxo-polyoxovanadium clusters  $[V_6O_7(OR)_{12}]$  ( $R = -CH_3, -C_2H_5$ ) are exceptional due to the fact that they carry no charge. Thus, despite their relatively high molecular weights ( $\sim 790$  and  $960$   $g \cdot mol^{-1}$ , respectively), their mass spectra show that they can

be sublimated without degradation upon heating in high vacuum.  $[V_6O_7(OCH_3)_{12}]$  has already been the object of an extensive investigation, proving particularly stable and showing a rich ion chemistry in the gas phase upon electrospray ionization.<sup>14</sup> Due to this feature, in combination with the clusters' magnetic and electrochemical properties, these substances could prove of great interest for applications in the surface sciences and heterogeneous catalysis research.

The most prominent feature displayed by these compounds, however, is certainly their large number of stable redox derivatives. With the exception of the iso-valent compounds comprising vanadium(+IV) centers, the clusters are all mixed-valent and, as such, are unique specimens for the investigation of electron delocalization in the highly symmetric hexanuclear core. A separate chapter is devoted to this particularly interesting topic, in which results from electrochemical, X-ray structural, and IR-spectroscopic investigations will be discussed in detail.

## Experimental Section

Reagent-grade chemicals were used in all reactions.  $VO(O^tBu)_3$  and  $VO(OC_2H_5)_3$  were prepared according to literature procedure.<sup>15</sup> Dichloromethane used in oxidation reactions with chlorine and  $SbCl_5$  was thoroughly dried with  $CaH_2$  and stored over molecular sieves (0.3 nm) prior to use.

For stoichiometric reactions, chlorine was condensed under reduced pressure ( $\sim 100$  mbar) into a graduated capillary held at liquid nitrogen temperature, and thawed at  $-78$  °C before further transfer by condensation into the reaction vessel.

Reactions under solvothermal conditions were conducted in pressure digestion vessels (Berghof, DAB 2) containing 50-mL Teflon inserts.

Column chromatography was performed on 63–200 mesh silica gel (Merck). Silica gel 60 TLC aluminum sheets (Merck) were used for thin-layer chromatography.

Extracted solutions containing reaction products were generally filtered, until clear, through a syringe filter (Roth, Rotilabo, PTFE, 0.2  $\mu m$ ) prior to crystallization.

**Preparation of  $N(n-C_4H_9)_4[V_6O_7(OCH_3)_{12}]$ .** In a 50-mL Teflon-lined pressure digestion vessel were heated 1.43 g (5 mmol) of  $VO(O^tBu)_3$ , 215 mg (0.83 mmol) of  $N^nBu_4[BH_4]$ , and 25 mL of methanol for 24 h at 125 °C. The resulting green solution was concentrated to approximately half its volume and stored overnight at  $-30$  °C, yielding dark green, needle shaped crystals of  $N(n-C_4H_9)_4[V_6O_7(OCH_3)_{12}] \cdot CH_3OH$ . The crystals were collected from the cold solution on a fritted filter funnel and thoroughly vacuum-dried, thus removing excess methanol. The work up of the solution was repeated with the filtrate in order to improve the yield to 80%.

Elemental analysis calcd (%) for  $C_{28}H_{72}NO_{19}V_6$  ( $M = 1032.52$  g/mol): C 32.57, H 7.03, N 1.36; found: C 32.40, H 6.94, N 1.26.

IR (KBr pellet,  $cm^{-1}$ ): 1172 (w), 1146 (vw), 1051 (vs), 957 (vs), 883 (vw), 802 (vw), 737 (vw), 693 (vw), 586 (vs), 431 (s), 408 (s).

**Preparation of  $[V_6O_7(OCH_3)_{12}]$  (1).**  $N(n-C_4H_9)_4[V_6O_7(OCH_3)_{12}]$  (500 mg, 0.484 mmol) and  $I_2$  (62 mg, 0.244 mmol) were dissolved in 50 mL of acetonitrile and stirred for 1 h. The reaction solution was then evacuated to dryness. The residue was extracted with  $3 \times 50$  mL of hexane, and the extract was then concentrated and stored at  $-30$  °C, yielding black octahedral crystals of **1**. The crystals were collected from the cold solution and air-dried (yield: 39%).

(9) Lindqvist, I. *Ark. Kemi* **1953**, *5*, 247–250.

(10) Spandl, J.; Daniel, C.; Brüdgam, I.; Hartl, H. *Angew. Chem., Int. Ed.* **2003**, *42*, 1163–1166.

(11) Lu et al. reported a vanadomolybdenum polyoxocation (Yang, W. B.; Lu, C. Z.; Zhan, X.; Zhuang, H. H. *Inorg. Chem.* **2002**, *41*, 4621–4623) of which the exact charge determination, however, has not been adequately demonstrated, in our opinion.

(12) (a) Khan, M. I.; Tabussum, S.; Doedens, R. J.; Golub, V. O.; O'Connor, C. C. *Inorg. Chem.* **2004**, *43*, 5850–5859. (b) Castro, S. L.; Sun, Z.; Bollinger, J. C.; Hendrickson, D. N.; Christou, G. *J. Chem. Soc., Chem. Commun.* **1995**, *24*, 2517–2518. (c) Chae, H. K.; Klemperer, W. G.; Páez Loyo, D. E.; Day, V. W.; Eberspacher, T. A. *Inorg. Chem.* **1992**, *31*, 3187–3189.

(13) We hereby, however, only consider polyoxometalates and their derivatives as truly cationic when the overall positive charge solely results from the metal centers and is not, for example, due to positive groups which are covalently tethered to a negatively charged polyoxometalate core: Ng, C. H.; Lim, C. W.; Teoh, S. G.; Fun, H.-K.; Usman, A.; Ng, S. W. *Inorg. Chem.* **2002**, *41*, 2–3.

(14) Schröder, D.; Engeser, M.; Brönstrup, M.; Daniel, C.; Spandl, J.; Hartl, H. *Int. J. Mass Spectrom.* **2003**, *228*, 743–757.

(15) Prandtl, W.; Hess, L. Z. *Anorg. Chem.* **1913**, *82*, 103–129.

Elemental analysis calcd (%) for  $C_{12}H_{36}O_{19}V_6$  ( $M = 790.04$  g/mol): C 18.24, H 4.59; found: C 18.22, H 4.48.

IR (KBr pellet,  $cm^{-1}$ ): 1170 (w), 1142 (w), 1032 (vs), 1019 (sh), 974 (vs), 692 (vw, broad), 585 (vs), 501 (w), 436 (s), 409 (vs).

MS (EI, 80 eV):  $m/z$  (%) = 790 (60)  $[M]^+$ , 630 (32)  $[M - VO(OCH_3)_3]^+$ , 470 (100)  $[M - 2VO(OCH_3)_3]^+$ .

**Preparation of  $[V_6O_7(OCH_3)_{12}][SbCl_6]$  (**2**).** All steps were carried out under inert conditions using Schlenk techniques. Into a 100-mL Schlenk tube were given 500 mg (0.633 mmol) of **1** and 0.09 mL (0.710 mmol) of  $SbCl_5$ . Fifty milliliters of dichloromethane and 20  $\mu$ L (0.907 mmol) of  $Cl_2$  were then successively condensed under reduced pressure into the Schlenk tube held at liquid nitrogen temperature. The reaction mixture was thawed to  $-78$  °C and slowly allowed to warm to room temperature while stirring. The solution was then evaporated to dryness and the residue extracted with  $5 \times 50$  mL anhydrous acetonitrile. The solution was concentrated under reduced pressure and stored for 3 d at  $-30$  °C yielding black, rod-shaped crystals of **2** (yield: 67%).

Elemental analysis calcd (%) for  $C_{12}H_{36}O_{19}Cl_6V_6Sb$  ( $M = 1124.53$  g/mol): C 12.82, H 3.23; found: C 12.71, H 3.10.

IR (KBr pellet,  $cm^{-1}$ ): 1170 (w), 1138 (vw), 1006 (vs), 991 (vs), 801 (vw), 710 (vw), 603 (s), 472 (vw), 446 (m), 421 (s).

**Preparation of  $[V_6O_7(OC_2H_5)_{12}]$  (**3**).** In a 50-mL Teflon-lined pressure digestion vessel were heated 0.89 mL (5 mmol) of  $VO(OC_2H_5)_3$ , 210 mg (0.82 mmol) of  $N^tBu_4[BH_4]$ , and 25 mL of ethanol for 24 h at 125 °C. The product of the solvothermal reaction was evaporated to dryness under reduced pressure, and the crude product was extracted with  $2 \times 20$  mL dichloromethane. The extract was evaporated to dryness under reduced pressure, and the residue was chromatographed on a silica gel column (elution with hexane/acetone, 2:1 by volume). The first fraction ( $R_f$  0.61) was evaporated to dryness, and the black residue was extracted with hexane until the extracting solution remained nearly colorless. The solution was concentrated under reduced pressure and stored at  $-30$  °C, yielding black, rhombohedral crystals of **3**, which were filtered off from the cold solution and air-dried (yield: 36%).

Elemental analysis calcd (%) for  $C_{24}H_{60}O_{19}V_6$  ( $M = 958.37$  g/mol): C 30.08, H 6.31; found: C 29.98, H 6.18.

IR (KBr pellet,  $cm^{-1}$ ): 1157 (w), 1089 (s), 1040 (vs), 972 (vs), 891 (s), 805 (w), 595 (s), 482 (w), 412 (s).

MS (EI, 80 eV):  $m/z$  (%) = 958 (19)  $[M]^+$ , 756 (16)  $[M - VO(OC_2H_5)_3]^+$ , 666 (22)  $[M - VO(OC_2H_5)_3 - 2OC_2H_5]^+$ , 554 (100)  $[M - 2VO(OC_2H_5)_3]^+$ .

**Preparation of  $[V_6O_7(OC_2H_5)_{12}][SbCl_6]$  (**4**).** All steps were carried out under inert conditions using Schlenk techniques. Into a 25-mL Schlenk tube were given 100 mg (0.104 mmol) of **3** and 13.2  $\mu$ L (0.104 mmol) of  $SbCl_5$ . Dichloromethane (15 mL) and  $Cl_2$  (10  $\mu$ L, 0.45 mmol) were then successively condensed under reduced pressure into the Schlenk tube held at liquid nitrogen temperature. The reaction mixture was thawed to  $-78$  °C and slowly allowed to warm to room temperature while stirring. The reaction solution was evacuated to dryness and the residue extracted with  $2 \times 20$  mL anhydrous dichloromethane. The solution was slightly concentrated under reduced pressure and stored at  $-30$  °C, yielding black crystals of **4** (yield: 53%).

Elemental analysis calcd (%) for  $C_{24}H_{60}O_{19}Cl_6V_6Sb$  ( $M = 1292.84$  g/mol): C 22.30, H 4.68; found: C 22.17, H 4.54.

IR (KBr pellet,  $cm^{-1}$ ): 1153 (w), 1086 (m), 1018 (vs), 983 (vs), 884 (s), 606 (s), 490 (w, broad), 416 (s).

**Preparation of  $[V_6O_7(OC_2H_5)_{12}][SbCl_6]_2$  (**5**).** All steps were carried out under inert conditions using Schlenk techniques. Into a 25-mL Schlenk tube were given 96 mg (0.1 mmol) of **3** and 26  $\mu$ L (0.205 mmol) of  $SbCl_5$ . Dichloromethane (15 mL) and  $Cl_2$  (10  $\mu$ L, 1.133 mmol) were then successively condensed under reduced pressure into the Schlenk tube held at liquid nitrogen temperature. The reaction mixture was thawed to  $-78$  °C and slowly allowed to warm to room temperature while stirring. The reaction solution was evacuated to dryness and the residue extracted with  $2 \times 20$  mL anhydrous

dichloromethane. The solution was slightly concentrated under reduced pressure and stored at  $-30$  °C, yielding black crystals of **5** (yield: 76%).

Elemental analysis calcd (%) for  $C_{24}H_{60}O_{19}Cl_{12}V_6Sb_2$  ( $M = 1627.31$  g/mol): C 17.71, H 3.72; found: C 17.63, H 3.59.

IR (KBr pellet,  $cm^{-1}$ ): 1150 (w), 1084 (m), 1006 (vs), 984 (vs), 868 (s), 610 (s), 493 (w, broad), 420 (m).

**X-ray Structure Analysis.** Single-crystal diffractometry was conducted on a Bruker XPS diffractometer (CCD area detector, Mo  $K\alpha$  radiation,  $\lambda = 0.71073$  Å, graphite monochromator). Single crystals of air-sensitive substances and of substances containing solvate molecules were taken directly out of the mother liquor and prepared under a cold nitrogen stream. Empirical absorption correction was applied on the data using symmetry-equivalent reflections (SADABS). The structures were solved using direct methods<sup>16</sup> and refined based on  $F^2$  data with a least-squares procedure<sup>17</sup> using the WinGX program system.<sup>18</sup> Anisotropic displacement parameters were assigned to all non-H atoms. The hydrogen atoms were calculated in geometrically idealized positions. Crystallographic data for compounds **1–5** at 173 K is summarized in Table 1.

**IR Spectroscopy.** IR spectra were collected in the 400–4000  $cm^{-1}$  region on a Nicolet 5 SXC FTIR spectrometer. The data was processed using the OMNIC E.S.P software (version 4.1 b).

**Cyclic Voltammetry.** Cyclovoltammetric investigations were carried out in a gastight three-electrode cell equipped with platinum wire working, counter, and pseudoreference electrode. The cell was connected to a computer-controlled potentiostat/galvanostat from EG&G Princeton Applied Research (model 173). The measurements were conducted in anhydrous dichloromethane with tetrabutylammonium hexafluorophosphate as a supporting electrolyte (0.1 M) and a working concentration of approximately  $10^{-3}$  mol·L<sup>-1</sup>. Redox potentials were referenced against the ferrocene/ferrocenium-couple.

The measurement data was processed with Microcal Origin (version 5.0).

**DSC.** Measurements were conducted in a Netzsch DSC 200 differential scanning calorimeter.

**MS.** The EI-MS experiments were conducted on a high-resolution MAT 711 mass spectrometer (Varian).

## Results and Discussion

**Solvothermal Synthesis.** The solvothermal syntheses of the  $\mu_6$ -oxo-dodeca- $\mu$ -alkoxo-hexa(oxovanadium) clusters  $[V_6O_7(OR)_{12}]$  ( $R = -CH_3, -C_2H_5$ ) represent a synthetic constraint in the sense that they are self-assembly processes<sup>19</sup> which have little in common with rational synthesis. It is a powerful method for synthesizing new compounds, yet the control (solvent, concentration, temperature, pressure, reaction time, etc.) over the products it yields is limited, and rarely straightforward. Thus, we have recently discovered that the synthesis of  $[V_6O_7(OCH_3)_{12}]$  (**1**) earlier reported,<sup>10</sup> consisting in the solvothermal reaction of  $VO(O^tBu)_3$  in methanol, offers a major side product which, being almost identical in composition and structure to **1**, was very difficult to detect and had therefore eluded our attention until now. For this reason we elaborated an alternative route for the synthesis of **1** via its singly reduced species. The latter is obtained in good yield and in high purity by solvothermal reaction of  $VO(O^tBu)_3$  and tetrabutylammonium boro-

(16) (a) *SHELXS-97*; A program for automatic solution of crystal structures; G. M. Sheldrick, University of Göttingen, Germany, 1997; Release 97-2. (b) Altomare, A.; Gasciarano, G.; Giacovazzo, C.; Gualardi, A. *J. Appl. Crystallogr.* **1993**, *26*, 343–350.

(17) *SHELXL-97*; A program for crystal structure refinement; G. M. Sheldrick, University of Göttingen, Germany, 1997; Release 97-2.

(18) Farrugia, L. J. *J. Appl. Crystallogr.* **1999**, *32*, 837–838.

(19) Khan, M. I.; Zubieta, J. *Prog. Inorg. Chem.* **1995**, *43*, 13–16 and references therein.

**Table 1.** X-ray Crystallographic Data for Compounds 1–5

compound	1	2	3	3 <sup>295K</sup>	4	5·2 CH <sub>2</sub> Cl <sub>2</sub>
formula	C <sub>12</sub> H <sub>36</sub> O <sub>19</sub> V <sub>6</sub>	C <sub>12</sub> H <sub>36</sub> O <sub>19</sub> Cl <sub>6</sub> V <sub>6</sub> Sb	C <sub>24</sub> H <sub>60</sub> O <sub>19</sub> V <sub>6</sub>	C <sub>24</sub> H <sub>60</sub> O <sub>19</sub> V <sub>6</sub>	C <sub>24</sub> H <sub>60</sub> O <sub>19</sub> Cl <sub>6</sub> V <sub>6</sub> Sb	C <sub>26</sub> H <sub>64</sub> O <sub>19</sub> Cl <sub>16</sub> V <sub>6</sub> Sb <sub>2</sub>
fw	790.05	1124.53	958.37	958.37	1292.85	1797.19
measured temperature (K)	173	173	173	295	173	173
crystal morph.	octahedron	rod-shaped	rhombohedron	rhombohedron	trigonal pyramid	octahedron
crystal size (mm × mm × mm)	0.5 × 0.3 × 0.2	0.17 × 0.08 × 0.07	0.4 × 0.4 × 0.3	0.44 × 0.35 × 0.26	0.27 × 0.16 × 0.11	0.45 × 0.32 × 0.25
crystal system	orthorhombic	hexagonal	monoclinic	trigonal	triclinic	triclinic
space group	<i>Pna</i> 2 <sub>1</sub>	<i>R</i> $\bar{3}$	<i>P</i> 2 <sub>1</sub> / <i>n</i>	<i>R</i> $\bar{3}m$	<i>P</i> $\bar{1}$	<i>P</i> $\bar{1}$
cell dimensions						
<i>a</i> (Å)	20.8343(12)	13.943(4)	10.338(4)	17.5332(15)	10.4567(17)	11.1503(19)
<i>b</i> (Å)	10.0830(6)	13.943(4)	17.760(8)	17.5332(15)	10.5469(17)	11.584(2)
<i>c</i> (Å)	13.5064(8)	16.773(6)	11.002(5)	11.224(2)	10.6194(17)	12.829(2)
$\alpha$ (deg)	90.00	90.00°	90.00	90.00	88.751(4)	109.445(3)
$\beta$ (deg)	90.00	90.00°	106.408(8)	90.00	86.169(4)	102.351(4)
$\gamma$ (deg)	90.00	120.00°	90.00	120.00	88.269(4)	93.771(4)
cell volume (Å <sup>3</sup> )	2837.3(3)	2823.8(15)	1937.7(14)	2988.2(6)	1167.8(3)	1509.3(5)
formula units <i>Z</i>	4	3	2	3	1	1
$\rho_{\text{calc}}$ (g/cm <sup>-3</sup> )	1.850	1.984	1.643	1.598	1.838	1.977
$\mu$ (Mo K $\alpha$ ) (mm <sup>-1</sup> )	1.971	2.621	1.459	1.419	2.125	2.534
abs. corr., <i>T</i> <sub>min</sub> / <i>T</i> <sub>max</sub>	0.41/0.65	0.67/0.81	0.74/1.00	0.68/0.87	0.84/1.00	0.86/1.00
$\theta_{\text{min}}/\theta_{\text{max}}$ (deg)	1.95/30.03	2.08/30.55	2.24/27.58	2.26/23.25	1.92/30.53	1.74/30.51
collected reflections	32332	11659	19107	7026	14662	18865
unique reflections	8265	1923	4489	530	7019	9070
ls parameters	348	95	229	69	290	319
R1 [ <i>I</i> > 2 $\sigma$ ( <i>I</i> )]	0.0282	0.0359	0.0494	0.0400	0.0336	0.0180
wR2 [ <i>I</i> > 2 $\sigma$ ( <i>I</i> )]	0.0694	0.0949	0.1211	0.1126	0.0747	0.0411
R1 (all data)	0.0347	0.0690	0.0586	0.0588	0.0523	0.0221
wR2 (all data)	0.0727	0.1087	0.1277	0.1304	0.0825	0.0423
GoF	1.017	0.889	1.116	1.075	1.028	1.034
larg. diff. $\pm$ (e $\cdot$ Å <sup>-3</sup> )	0.54/−0.31	0.37/−1.05	1.45/−0.51	0.30/−0.22	1.00/−0.42	0.49/−0.47

hydride in methanol.<sup>20</sup> **1** is then easily obtained by oxidation of  $N(n\text{-C}_4\text{H}_9)_4[\text{V}_6\text{O}_7(\text{OCH}_3)_{12}]$  with iodine.

$[\text{V}_6\text{O}_7(\text{OC}_2\text{H}_5)_{12}]$  (**3**) is synthesized by solvothermal reaction of  $\text{VO}(\text{OC}_2\text{H}_5)_3$  and tetrabutylammonium borohydride in ethanol. Unlike methanol, under the solvothermal conditions employed, ethanol is not sufficiently reducing to generate vanadium(+IV) necessary for the synthesis of **3**, which like **1** contains four V<sup>IV</sup> ions. Thus, borohydride is employed as a reducing agent in this reaction.

An account, however, exists of the inadvertent formation of  $[\text{V}_6\text{O}_7(\text{OC}_2\text{H}_5)_{12}]$  (**3**), apparently by microhydrolysis of  $\text{VO}(\text{OC}_2\text{H}_5)_3$  during the shipping procedure of a damaged flask of the chemical.<sup>21</sup> This could however not serve as a basis for a general synthetic procedure of the substance.

**Electrochemistry and Redox Reactions.** The neutral clusters **1** and **3** contain VO<sub>6</sub> octahedra comprising one terminal oxygen atom respectively, classifying them according to Pope as type-I polyanion-derivatives.<sup>22</sup> In the absence of in-plane bonding, the LUMO for type-I polyhedra is a nominally nonbonding, mainly metal-centered “d<sub>xy</sub>” orbital.<sup>1b</sup> Accordingly, this class of polyoxometalates allows the reversible uptake of a number of electrons, which populate the predominantly nonbonding d<sub>xy</sub>-orbital in the metal centers. As a result, the compounds retain their initial structures to a large extent, only minor changes taking place upon reduction.<sup>1a</sup>

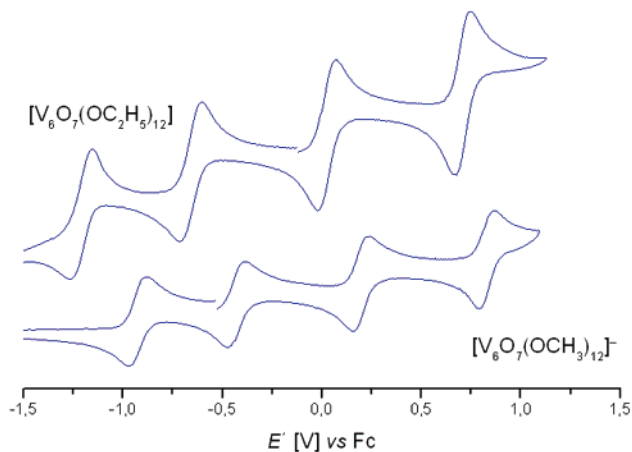


**Figure 2.** Cyclic voltammograms of **1**<sup>−</sup> (tetrabutylammonium salt) and **3** measured in dichloromethane and referenced against the ferrocene/ferrocenium couple.

Accordingly, the cyclic voltammograms of the cluster compounds  $[\text{V}^{\text{IV}}_5\text{V}^{\text{V}}_1\text{O}_7(\text{OCH}_3)_{12}]^-$  (**1**<sup>−</sup>) and  $[\text{V}^{\text{IV}}_4\text{V}^{\text{V}}_2\text{O}_7(\text{OC}_2\text{H}_5)_{12}]$  (**3**) shown in Figure 2 display four reversible single-electron transfers, spanning a row of five isostructural hexavanadium compounds with varying V<sup>IV</sup> content respectively, ranging from the isostructural alkoxo-polyoxovanadate dianion  $[\text{V}^{\text{IV}}_6\text{O}_7(\text{OR})_{12}]^{2-}$  up to the dicationic  $[\text{V}^{\text{IV}}_2\text{V}^{\text{V}}_4\text{O}_7(\text{OR})_{12}]^{2+}$  species. **1**<sup>−</sup> as its tetrabutylammonium salt was the substance of choice for the cyclovoltammetric investigation of the methoxo cluster series, giving the best cyclic voltammograms in regard to the criteria of reversibility and hence, providing the greatest accuracy in

(20) Spandl, J. Doctoral Thesis, Freie Universität, Berlin, Germany, 2001.

(21) Kessler, V. G.; Seisenbaeva, G. A. *Inorg. Chem. Commun.* **2000**, *3*, 203–204.

(22) Pope, M. T. *Inorg. Chem.* **1972**, *11*, 1973–1974.

**Table 2.** Redox Potentials Obtained from the Cyclic Voltammograms of Compounds **1**<sup>-</sup> (Tetrabutylammonium Salt) and **3**<sup>a</sup>

redox process	$E^0$ vs Fc in $\text{CH}_2\text{Cl}_2$ (V)	
	R = $-\text{CH}_3$	R = $-\text{C}_2\text{H}_5$
$[\text{V}^{\text{IV}}_3\text{V}^{\text{V}}_3\text{O}_7(\text{OR})_{12}]^+ \rightleftharpoons [\text{V}^{\text{IV}}_2\text{V}^{\text{V}}_4\text{O}_7(\text{OR})_{12}]^{2+} + e^-$	+0.83	+0.75
$[\text{V}^{\text{IV}}_4\text{V}^{\text{V}}_2\text{O}_7(\text{OR})_{12}] \rightleftharpoons [\text{V}^{\text{IV}}_3\text{V}^{\text{V}}_3\text{O}_7(\text{OR})_{12}]^+ + e^-$	+0.20	+0.03
$[\text{V}^{\text{IV}}_5\text{V}^{\text{V}}_1\text{O}_7(\text{OR})_{12}]^- \rightleftharpoons [\text{V}^{\text{IV}}_4\text{V}^{\text{V}}_2\text{O}_7(\text{OR})_{12}] + e^-$	-0.40	-0.66
$[\text{V}^{\text{IV}}_6\text{O}_7(\text{OR})_{12}]^{2-} \rightleftharpoons [\text{V}^{\text{IV}}_5\text{V}^{\text{V}}_1\text{O}_7(\text{OR})_{12}]^- + e^-$	-0.93	-1.21

<sup>a</sup>  $c = 5 \times 10^{-4}$  M; sweep rate = 50 mV/s.

**Table 3.** Comproportionation Constants  $K_c$  (298 K) for the  $[\text{V}_6\text{O}_7(\text{OR})_{12}]$ -Series<sup>a</sup>

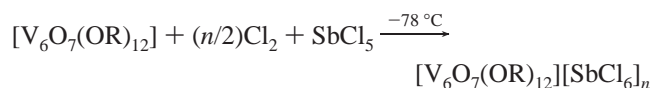
redox active cluster	R = $-\text{CH}_3$	R = $-\text{C}_2\text{H}_5$
$[\text{V}^{\text{IV}}_5\text{V}^{\text{V}}_1\text{O}_7(\text{OR})_{12}]^-$	$9.2 \times 10^8$	$2.0 \times 10^9$
$[\text{V}^{\text{IV}}_4\text{V}^{\text{V}}_2\text{O}_7(\text{OR})_{12}]$	$1.4 \times 10^{10}$	$4.7 \times 10^{11}$
$[\text{V}^{\text{IV}}_3\text{V}^{\text{V}}_3\text{O}_7(\text{OR})_{12}]^+$	$4.5 \times 10^{10}$	$1.5 \times 10^{12}$

<sup>a</sup>  $RT \ln K_c = nF(E^{0'}_1 - E^{0'}_2)$ .

determining the redox potentials. As a matter of course, the cyclic voltammogram of the neutral compound **1** affords identical redox potentials. The redox potentials obtained for the respective cluster series are listed in Table 2. As is to be expected, the greater positive inductive effect of the ethyl groups in the ethoxo series causes a shift in the respective single-oxidation potentials to more negative values as compared to those of **1**<sup>-</sup> and its redox isomers.<sup>23</sup>

The electrochemical potential separations between successive one-electron redox events  $\Delta E^{0'}$  in the cyclic voltammograms of **1**<sup>-</sup> and **3** are very large, ranging from 530 to 720 mV. These values correspond to large comproportionation constants<sup>24</sup>  $K_c \approx 10^9$ – $10^{12}$ , indicating high thermodynamic stability of the redox active species toward disproportionation to their one-electron oxidized and reduced derivatives, respectively (Table 3). These values are crucial for preparative chemistry, for they determine the feasibility of isolating a pure solid mixed-valence compound from its solution.<sup>25</sup>

Encouraged by these observations, our synthetic endeavor consisted in chemically producing and isolating all redox derivatives of **1** and **3**, particular interest being paid to the highly unusual cationic species. For the synthesis of the latter, we experimented with a variety of oxidants.<sup>26</sup> Oxidation by chlorine in the presence of antimony pentachloride finally proved to be particularly suitable for our purposes, due to the mixture's high oxidation potential as well as to the reactions' completeness and easy workup. In these reactions chlorine is generally used in large excess, the respective degree of oxidation being controlled by the stoichiometry of antimony pentachloride in the reaction mixture.  $\text{SbCl}_5$  acts as a Lewis acid, generating hexachloroantimonate as the counterion by complexing chloride formed in the oxidation:



Oxidation of **1** to the dicationic methoxo derivative  $[\text{V}^{\text{IV}}_2\text{V}^{\text{V}}_4\text{O}_7(\text{OCH}_3)_{12}]^{2+}$  with the  $\text{Cl}_2/\text{SbCl}_5$  mixture in dichloromethane was not successful. This species equally could not be chemically synthesized using very strong oxidizing agents such as  $\text{NO}_2[\text{SbF}_6]$  ( $E^{0'}$  vs Fc = +1.03 V in  $\text{CH}_2\text{Cl}_2$ ),<sup>27</sup> all of which only generated the monocationic species. The dicationic species should, however, be accessible through electrosynthesis.

**IR Spectroscopy.** IR spectroscopy is a very useful tool for the analysis of the alkoxo-polyoxovanadium clusters. Particularly the 400–1200  $\text{cm}^{-1}$  region is of interest, containing absorption bands due to metal–oxygen stretching vibrations which are characteristic of polyoxometalate spectra in general. The assignment of the vibration modes in this region was tentatively conducted on the basis of normal coordinate analyses and vibrational investigations on Lindvist anions<sup>28</sup> as well as by comparison with IR data from related alkoxo-polyoxovanadates containing the  $\{\text{V}_6\text{O}_{19}\}$  core.<sup>23,29</sup>

The clusters of the general formula  $[\text{V}^{\text{IV}}_n\text{V}^{\text{V}}_{6-n}\text{O}_7(\text{OR})_{12}]^{(4-n)}$  presented here have the advantage of containing only one type of  $\mu$ -bridging ligand, which greatly simplifies their IR spectra. If care is taken that the salts do not contain coordinating counterions, then the charged species' spectra compare quite well with those of the neutral compounds. This afforded a convincing assignment of the most important stretching vibrations in the dodeca-alkoxo-oxo-hexa(oxovanadium) clusters' IR spectra.

The spectra are thus best characterized by four absorption bands in the 400–1200  $\text{cm}^{-1}$  region. The two most prominent are located in the 950–1100  $\text{cm}^{-1}$  region: the  $\text{O}_b$ –R (1000–1100  $\text{cm}^{-1}$ ) and the V– $\text{O}_t$  (950–1000  $\text{cm}^{-1}$ ) stretching modes. The absorption band in the 550–650  $\text{cm}^{-1}$  region can be attributed to V– $\text{O}_b$ –V bending, and one in the 400–450  $\text{cm}^{-1}$  region to V– $\text{O}_c$  stretching, the central oxygen atom vibrating within the octahedral vanadium framework.<sup>28a</sup>

All four vibration modes are sensitive to the cluster's overall charge, the  $\text{O}_b$ –R and V– $\text{O}_t$  stretching showing the greatest dependency. The species with higher d-electron content show higher  $\text{O}_b$ –R stretching frequencies due to the larger negative partial charge on the bridging oxygen atoms, which increases the polarity and thus the strength of the O–CH<sub>3</sub> bond. On the other hand, the smaller positive charge on the vanadium atoms in these species diminishes the polarity of the bonds to the respective terminal oxygen atoms, the V– $\text{O}_t$  stretching vibration thus shifting to lower frequencies upon reduction of the cluster. The cluster charge-to-frequency relationship for these vibration modes is displayed in Figure 3, based on spectral data obtained from the neutral compounds as well as from their redox derivatives' tetrabutylammonium<sup>30</sup> and hexachloroantimonate salts, respectively. The relationship is of great practical use since it allows the rapid and unambiguous determination of a cluster's charge from IR spectroscopic data. This easily accessible and reliable information makes the method highly useful for analyzing reaction mixtures and products.

One further aspect of the clusters' IR spectra, which will prove of great importance for the discussion on mixed valency

- (23) Chen, Q.; Goshorn, D. P.; Scholes, C. P.; Tan, X.; Zubieta, J. *J. Am. Chem. Soc.* **1992**, *114*, 4667–4681.  
 (24) Richardson, D. E.; Taube, H. *Inorg. Chem.* **1981**, *20*, 1278–1285.  
 (25) Ludi, A. In *Mixed-Valence Compounds: Theory and Applications in Chemistry, Physics, Geology, and Biology*; Brown, D. B., Ed.; D. Reidel Publishing Company: Dordrecht, 1980; 33.  
 (26) Connelly, N. G.; Geiger, W. E. *Chem. Rev.* **1996**, *96*, 877–910.

- (27) Kochi, J. K. *Acc. Chem. Res.* **1992**, *25*, 44.  
 (28) (a) Rocchiccioli-Deltcheff, C.; Thouvenot, R.; Fouassier, M. *Inorg. Chem.* **1982**, *21*, 30–35. (b) Mattes, R.; Bierbüsse, H.; Fuchs, J. *Z. Anorg. Allg. Chem.* **1971**, *385*, 230–242.  
 (29) (a) Hou, D.; Kim, G.-S.; Hagen, K. S.; Hill, K. L. *Inorg. Chim. Acta* **1993**, *211*, 127–130. (b) Khan, M. I.; Chen, Q.; Höpe, H.; Parkin, S.; O'Connor, C. J.; Zubieta, J. *Inorg. Chem.* **1993**, *32*, 2929–2937.  
 (30) Spandl, J.; Daniel, C.; Brüdgam, I.; Hartl, H. *Angew. Chem., Int. Ed.* **2003**, *42*, Supporting Information.

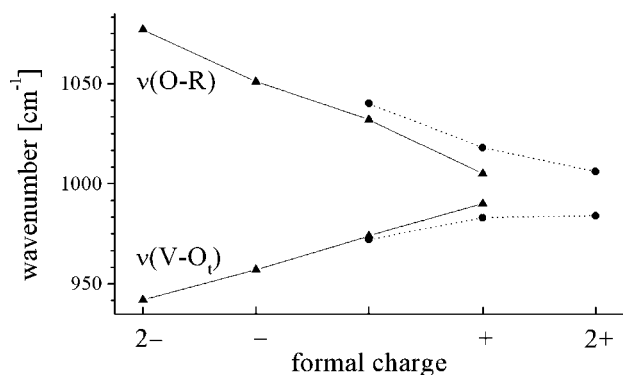


**Figure 3.** Charge ( $n$ ) to wavenumber dependency for the  $\nu(\text{O}_b\text{-R})$  and  $\nu(\text{V-O}_i)$  vibration modes in the  $[\text{V}_6\text{O}_7(\text{OCH}_3)_{12}]^{n+}$  (▲) and  $[\text{V}_6\text{O}_7(\text{OC}_2\text{H}_5)_{12}]^{n+}$  (●) IR spectra respectively (KBr pellet).

and electron delocalization below, concerns their simplicity. In the 500–1000  $\text{cm}^{-1}$  region, the spectra only show two absorption bands: one for the  $\text{V-O}_i$  stretching and one for the  $\text{V-O}_b\text{-V}$  bending vibration, respectively. Other symmetrically substituted polyoxometalate derivatives comprising the hexavanadate core<sup>29b,31</sup> all display additional vibration modes in this region. This directly reflects the high symmetry found in the dodeca-alkoxo cluster series, the number of bands in the metal–oxygen stretching region comparing well with those found in the IR spectra of Lindqvist anions.<sup>28</sup>

### Mixed Valency

As in mixed-valence compounds in general, the unpaired electrons in the alkoxo-polyoxovanadium clusters can either be localized or delocalized. In the event of delocalization, it may concern selected or all metal centers. Theoretical and experimental investigation of electron delocalization in the hexametalate core<sup>1a,32,33b–d</sup> and in polyoxometalates,<sup>1a,33</sup> as well as in mixed-valence compounds in general,<sup>34</sup> is an area of research of considerable interest for which several models have been proposed.<sup>35</sup>

The widely accepted classification scheme proposed by Robin and Day for mixed-valence compounds<sup>36</sup> focuses on the degree of electronic interaction present between sites of differing valence and the ensuing charge delocalization. Three levels of delocalization are proposed, ranging from localized (class I) to completely delocalized (class III), class II representing compounds which, depending on their condition and the method of

measurement involved, display features typical for both localized and delocalized states, as well as for states which can be considered as intermediate to these.

Class II compounds are of particular interest since they are excellent models for investigating the mechanisms of electron transfer. Thus, the factors which influence the transition (temperature, solvate, ligand sphere, transition metal, etc.) can be varied in numerous ways, delivering detailed information on the extent to which a given variable influences the intervalence charge transfer (IVCT). Furthermore, depending on the time scale of the method of investigation involved, the exchange rate  $k_{\text{ET}}$  can be estimated.<sup>34a</sup>

In the past decades, research on mixed valency has focused on polynuclear transition metal complexes, among which the Creutz–Taube ion is certainly the most prominent example.<sup>37</sup> Although a large number of mixed-valence complexes exist, attention has mainly been paid to those possessing a high point symmetry, since their mixed-valence centers have identical site symmetry in the respective oxidation states. In these compounds the localized states have the same energy, thus greatly simplifying their theoretical modeling,<sup>35b</sup> which is an important prerequisite for the correct interpretation of experimental results.

The Lindqvist structure (Figure 1) is predestined for the investigation of mixed valency in polynuclear transition metal complexes due to the high symmetry found in the hexametalate core. Research has been conducted on the reduced molybdenum and tungsten isopolyanions,<sup>1a,33c,38</sup> which, however, can only take up two electrons, respectively. The metal centers in the structure describe an octahedron and possess  $C_{4v}$  site symmetry respectively, a situation which, as IR-spectroscopic results suggest (vide supra), is to a large extent also valid for  $\mu$ -substituted dodeca-alkoxo-oxo-hexa(oxovanadium) cluster derivatives comprising monodentate alkoxo ligands. This condition is not fulfilled in other hexavanadium derivatives containing either different  $\mu$ -bridging ligands,<sup>8</sup> bridging trisalkoxo,<sup>39</sup> or organometallic fragments<sup>31</sup> as bridging ligands.

The series of alkoxo-polyoxovanadium clusters presented here and in a previous publication<sup>10</sup> have properties which distinguish them for mixed-valence research. Besides the symmetry requirements they fulfill, they can accept up to six electrons without engaging in metal–metal bonds as shown from the interatomic vanadium distances obtained by X-ray structure analysis. Hence, a large number of mixed-valence states in a highly symmetric hexametalate core can be realized, all of which, as cyclovoltammetric investigations have disclosed (vide supra), are remarkably stable.

The following subsections address the subject of mixed valency in the clusters presented in this work, within the boundaries of the experimental methods used and their respective time scales.

- (31) (a) Hayashi, Y.; Ozawa, Y.; Isobe, K. *Chem. Lett.* **1989**, 425. (b) Chae, H. K.; Klemperer, W. G.; Day, V. W. *Inorg. Chem.* **1989**, 28, 1423. (c) Hayashi, Y.; Ozawa, Y.; Isobe, K. *Inorg. Chem.* **1991**, 30, 1025–1033.
- (32) (a) Bridgeman, A. J.; Cavigliasso, G. *Inorg. Chem.* **2002**, 41, 1761–1770 and references therein. (b) Augustyniak-Jablokow, M. A.; Borshch, S. A.; Daniel, C.; Hartl, H.; Yablokov, Y. V. *New J. Chem.* **2005**, 29, 1064–1071.
- (33) (a) Pope, M. T. In *Comprehensive Coordination Chemistry II*; McCleverty, J. A., Meyer, T. J., Eds.; Elsevier: Oxford 2004; Vol. 4, pp 663–667 and references therein. (b) Pope, M. T. In *Mixed-Valence Compounds: Theory and Applications in Chemistry, Physics, Geology, and Biology*; Brown, D. B., Ed.; D. Reidel Publishing Company: Dordrecht, 1980; pp 365–386. (c) Sanchez, C.; Livage, J.; Launay, J. P.; Fournier, M.; Jeannin, Y. *J. Am. Chem. Soc.* **1982**, 104, 3194–3202. (d) Piegras, K.; Barrows, J. N.; Pope, M. T. *J. Chem. Soc., Chem. Commun.* **1989**, 1, 10–12.
- (34) (a) Demadis, K. D.; Hartshorn, C. M.; Meyer, T. J. *Chem. Rev.* **2001**, 101, 2655–2685. (b) Prassides, K., Ed. *Mixed Valency Systems: Applications in Chemistry, Physics and Biology*; Kluwer: Dordrecht, 1991. (c) Brown, D. B., Ed. *Mixed-Valence Compounds: Theory and Applications in Chemistry, Physics, Geology, and Biology*; D. Reidel Publishing Company: Dordrecht, 1980. (d) Breedlove, B. K.; Yamaguchi, T.; Ito, T.; Londergan, C. H.; Kubiak, C. P. In *Comprehensive Coordination Chemistry II*; McCleverty, J. A.; Meyer, T. J., Eds.; Elsevier: Oxford 2004; Vol. 2, pp 717–729.

- (35) (a) Hush, N. S. In *Mixed-Valence Compounds: Theory and Applications in Chemistry, Physics, Geology, and Biology*; Brown, D. B., Ed.; D. Reidel Publishing Company: Dordrecht, 1980; pp 151–188. (b) Schatz, P. N. In *Inorganic Electronic Structure and Spectroscopy*; Solomon, E. I.; Lever, A. B. P., Eds.; John Wiley & Sons: New York, 1999; Vol. 2, pp 175–226 and references therein. (c) Creutz, C.; Newton, M. D.; Sutin, N. *J. Photochem. Photobiol., A* **1994**, 82, 47–59. (d) Hupp, J. T. In *Comprehensive Coordination Chemistry II*; McCleverty, J. A., Meyer, T. J., Eds.; Elsevier: Oxford 2004; Vol. 2, pp 709–716 and references therein.
- (36) Robin, M. P.; Day, P. *Adv. Inorg. Chem. Radiochem.* **1976**, 10, 247.
- (37) Creutz, C. *Prog. Inorg. Chem.* **1983**, 30, 1–73.
- (38) Pope, M. T. *Prog. Inorg. Chem.* **1991**, 39, 235–236.
- (39) Khan, M. I.; Chen, Q.; Zubieta, J.; Goshorn, D. P.; *Inorg. Chem.* **1992**, 31, 1556–1558.

**Cyclic Voltammetry.** Resolved one-electron redox processes in the cyclic voltammograms of mixed-valence compounds are a clear indication of electronic interaction between the redox-active sites. Ideally, molecules containing noninteracting centers display a multielectron transfer at one single potential,<sup>40</sup> whereas compounds with significant interaction between redox-active centers exhibit cyclic voltammograms with multiple single-electron transfers. Multielectron processes, however, can conceal unresolved single-electron events and therefore do not automatically exclude the possibility of weak electronic coupling.<sup>24</sup> Thus, the magnitude of  $\Delta E^{0'}$  between neighboring redox potentials is, among other factors of lower impact influencing the separation, representative of the stabilization energy imparted to the mixed-valence state by electron delocalization.<sup>41</sup>

The cyclic voltammograms of **1**<sup>-</sup> and **3** (Figure 2) display large potential separations  $\Delta E^{0'}$  between successive one-electron events (Table 2) compared to the values in other mixed-valence compounds.<sup>34d,41a,42</sup> There are, however, examples of systems with comparable potential separations comprising bridging ligands mediating very strong electronic coupling.<sup>43</sup> A large  $\Delta E^{0'}$  is also found for hexamolybdate,<sup>38</sup> which, however, as is the case for the tungsten analogon, cannot be reduced further than its two-electron reduction product.<sup>1a</sup> Hence, the dodeca-alkoxo-oxo-hexa(oxovanadium) cluster series exhibits substantial thermodynamic stabilization in all mixed-valence species detected in the cyclovoltammetric experiment, rendering the {V<sub>6</sub>O<sub>19</sub>} core an apparently ideal framework for paramagnetic electron delocalization.

The fact that all 12  $\mu$ -bridging oxo ligands of the Lindqvist structure are substituted by monodentate alkoxo ligands is essential for the ease of electron transfer, which is strongly correlated to the vanadium centers' site symmetry. Accordingly, polyoxovanadate derivatives of lower symmetry comprising the {V<sub>6</sub>O<sub>19</sub>} core exhibit cyclic voltammograms with only one<sup>23</sup> or at most two<sup>29b,44</sup> redox potentials with substantially smaller  $\Delta E^{0'}$  values, owing to the dissymmetry imposed by the differing ligands, as well as to the covalent tethering of the alkoxo groups in the chelating moieties. Furthermore, the influence of coordinating cations on a cluster's electrochemical properties should not be underestimated, which particularly in organic solvents can cause a strong distortion of symmetry and charge distribution.

The splitting of the redox potentials  $\Delta E^{0'}$  in the cyclic voltammograms of **1**<sup>-</sup> and **3** is associated with the thermodynamic stabilization of the chemical species involved in both redox events which define the gap (Table 2). Under the premises that electronic coupling between the vanadium sites and especially the stabilization energy arising from electron delocalization represent the major contributions to the size of  $\Delta E^{0'}$

**Table 4.** Valence Sum Calculations for the Crystallographically Independent Vanadium Atoms in Compounds **1–5** Based on X-ray Crystallographic Data Collected at 173 K

cluster/cluster ion (compound)	V <sup>IV</sup>	V <sup>V</sup>	bond-valence sums						
			V(1)	V(2)	V(3)	V(4)	V(5)	V(6)	
[V <sub>6</sub> O <sub>7</sub> (OCH <sub>3</sub> ) <sub>12</sub> ] ( <b>1</b> )	4	2	V <sup>IV</sup>	4.73	<b>4.14</b>	<b>4.14</b>	<b>4.17</b>	<b>4.12</b>	4.81
			V <sup>V</sup>	<b>4.98</b>	4.36	4.35	4.39	4.34	<b>5.06</b>
[V <sub>6</sub> O <sub>7</sub> (OC <sub>2</sub> H <sub>5</sub> ) <sub>12</sub> ] ( <b>3</b> )	4	2	V <sup>IV</sup>	<b>4.03</b>	4.68	<b>4.06</b>	—	—	—
			V <sup>V</sup>	4.24	<b>4.93</b>	4.28	—	—	—
[V <sub>6</sub> O <sub>7</sub> (OCH <sub>3</sub> ) <sub>12</sub> ] <sup>+</sup> ( <b>2</b> )	3	3	V <sup>IV</sup>	4.52	—	—	—	—	—
			V <sup>V</sup>	4.75	—	—	—	—	—
[V <sub>6</sub> O <sub>7</sub> (OC <sub>2</sub> H <sub>5</sub> ) <sub>12</sub> ] <sup>+</sup> ( <b>4</b> )	3	3	V <sup>IV</sup>	4.31	4.42	4.45	—	—	—
			V <sup>V</sup>	4.54	4.66	4.68	—	—	—
[V <sub>6</sub> O <sub>7</sub> (OC <sub>2</sub> H <sub>5</sub> ) <sub>12</sub> ] <sup>2+</sup> ( <b>5</b> )	2	4	V <sup>IV</sup>	4.73	4.28	4.50	—	—	—
			V <sup>V</sup>	<b>4.98</b>	4.50	4.74	—	—	—

(vide supra), the potential differences can be attributed to differing magnitudes of the latter in the mixed-valence species. Thus, the ethoxo derivatives generally display somewhat greater  $\Delta E^{0'}$  values compared to those of methoxo species comprising the same V<sup>IV</sup>/V<sup>V</sup> ratios. Within a cluster series,  $\Delta E^{0'}$  continually increases toward cluster species with smaller V<sup>IV</sup>/V<sup>V</sup> ratios, i.e., with decreasing d-electron content. Unfortunately, the  $\Delta E^{0'}$  value for neither of the dicationic species could be determined, the redox potential of the respective [V<sup>IV</sup><sub>2</sub>V<sup>V</sup><sub>4</sub>O<sub>7</sub>(OR)<sub>12</sub>]<sup>2+</sup>/[V<sup>IV</sup><sub>1</sub>V<sup>V</sup><sub>5</sub>O<sub>7</sub>(OR)<sub>12</sub>]<sup>3+</sup> redox pair lying beyond the limits of the measurement conditions employed in the cyclovoltammetric experiment. It would, however, be interesting to determine whether the trend to larger  $\Delta E^{0'}$  values continues, or if within the electron–hole analogy, the largest mixed-valence stabilization is realized for the “half-filled” cluster comprising a 3:3 V<sup>IV</sup>/V<sup>V</sup> ratio. CV experiments aiming at the acquisition of further redox transitions at highly positive potentials are currently in progress.

**Valence Sum Calculations.** X-ray structure analysis provides insight on mixed valency in the solid state, on a time scale which vastly exceeds the event of electron transfer and thus clearly shows delocalization. When in possession of good quality structural data, it is possible to calculate the valence sums of certain atoms to determine their oxidation state. This can furthermore be used to determine excess charge or charge deficit in atoms beyond their ideal valency, a practice which has found wide use in polyoxometalate chemistry.<sup>45</sup> In mixed-valence compounds, these calculations are useful for determining the oxidation state of the element in question. Deviations from whole number valences can be interpreted as arising from delocalization of the unpaired electron(s) to an extent which corresponds to the degree of the observed discrepancy.

The valence sum calculations presented here were performed on data from X-ray structure analysis obtained, unless otherwise stated, at 173 K. The bond valence parameters for V<sup>IV</sup> and V<sup>V</sup> as well as the “universal” constant *b* were taken from Brese and O'Keeffe.<sup>46</sup> Calculations were performed on crystallographically independent vanadium atoms for the valences +IV and +V, respectively. The results for compounds **1–5** are listed in Table 4.

Valence sum calculations conducted on the crystal structures of compounds **1–5** at 173 K yield different results as to the

- (40) Flanagan, J. B.; Shlomo, M.; Bard, A. J.; Anson, F. C. *J. Am. Chem. Soc.* **1978**, *100*, 4248–4253.
- (41) (a) Gagné, R. R.; Spiro, C. L. *J. Am. Chem. Soc.* **1980**, *102*, 1443–1444. (b) Crutchley, R. J. In *Comprehensive Coordination Chemistry II*; McCleverty, J. A.; Meyer, T. J., Eds.; Elsevier: Oxford 2004; Vol. 2, pp 235–244.
- (42) (a) Kreis, J.; Kirss, R. U.; Reiff, W. M. *Inorg. Chem.* **1994**, *33*, 1562–1565. (b) Richardson, D. E.; Taube, H. *Coord. Chem. Rev.* **1984**, *60*, 107–129. (c) Harmalkar, S. P.; Leparulo, M. A.; Pope, M. T. *J. Am. Chem. Soc.* **1983**, *105*, 4286–4292.
- (43) (a) Lay, P. A.; Magnuson, R. H.; Taube, H. *Inorg. Chem.* **1988**, *27*, 2364–2371. (b) Manriquez, J. M.; Ward, M. D.; Reiff, W. M.; Calabrese, J. C.; Jones, N. L.; Caroll, P. J.; Bunel, E. E.; Miller, J. S. *J. Am. Chem. Soc.* **1995**, *117*, 6182–6193.
- (44) Müller, A.; Meyer, J.; Bögge, H.; Stämmler, A.; Botar, A. Z. *Anorg. Allg. Chem.* **1995**, *621*, 1818–1831.

- (45) Tytko, K. H.; Mehmke, J.; Kurad, D. Fischer, S. *Bonding and Charge Distribution in Polyoxometalates: A Bond Valence Approach*; Mingos, D. M. P., Fischer, S., Eds.; Structure and Bonding, Vol. 93; Springer: Berlin, 1999; pp 1–66, 129–321.
- (46) Brese, N. E.; O'Keeffe, M. *Acta Crystallogr.* **1991**, *B47*, 192–197.



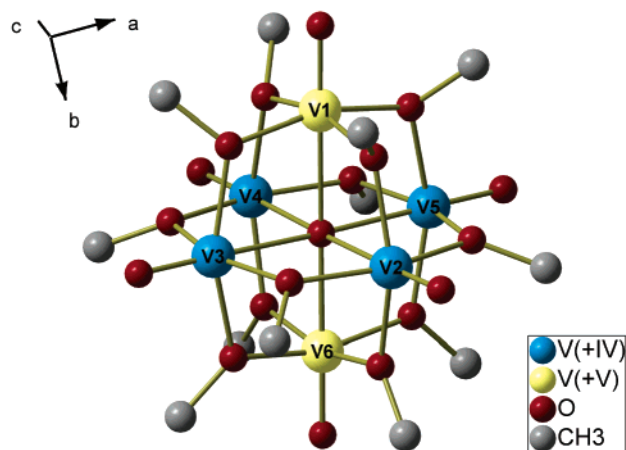


**Figure 4.** Crystal structure of  $[V^{IV}_4V^V_2O_7(OCH_3)_{12}]$  (**1**).

**Table 5.** Valence Sum Calculations for the Crystallographically Independent Vanadium Atoms in Compounds **1** and **3** Based on X-ray Crystallographic Data Collected at Room Temperature (295 K)

compound	$V^{IV}$	$V^V$	bond-valence sums						
			V(1)	V(2)	V(3)	V(4)	V(5)	V(6)	
$[V_6O_7(OCH_3)_{12}]$ ( <b>1</b> ) <sup>295K</sup>	4	2	$V^{IV}$	4.68	<b>4.12</b>	<b>4.20</b>	<b>4.10</b>	<b>4.13</b>	4.75
			$V^V$	<b>4.92</b>	4.34	4.42	4.32	4.34	<b>5.00</b>
$[V_6O_7(OC_2H_5)_{12}]$ ( <b>3</b> ) <sup>295K</sup>	4	2	$V^{IV}$	4.37	—	—	—	—	—
			$V^V$	4.60	—	—	—	—	—

delocalization of the d-electrons, depending on the  $V^{IV}/V^V$  ratio of a given compound. The neutral compounds **1** and **3** with a 2:1 ratio contain localized vanadium valences in the solid state, whereas the monocationic species **2** and **4** with a 1:1 ratio display complete delocalization of the three unpaired electrons (Table 4). The valence sums for the dicationic ethoxo cluster **5** with a 1:2 ratio indicate that both electrons are contained in one of the cluster's planar  $V_4O_4$  rings. This resembles the result obtained for **1** and **3**, respectively, in which all four unpaired electrons are located in a planar  $V_4O_4$  ring (Figure 4). It is not clear from the valence sums for compound **5**, however, whether the electrons are delocalized within the  $V_4O_4$  ring or if the mixed valency for these ions results from rotational disorder in the crystal structure.

Interestingly, upon temperature increase, the neutral ethoxo cluster **3** goes through a phase transition from the low-temperature monoclinic structure ( $P2_1/n$ ) at 173 K to the high-temperature trigonal modification ( $R\bar{3}m$ ) at 295 K (Table 1), leading to a structure at room temperature with the d-electrons delocalized over all six vanadium centers (Table 5). Differential scanning calorimetry (DSC) measurements indicate a hardly detectable phase transition at about 220 K. An analogous phase transition is not observed for the neutral methoxo cluster **1**, for which the X-ray structure analysis conducted at room temperature corresponds to the low-temperature data, showing the same results for the respective valence sums (Table 5). DSC measurements conducted on **1** between 153 and 323 K show no detectable phase transition.

Detailed studies of valence-trapping and -detrapping in molecular mixed-valence compounds in the solid state have been published, in which among other methods, X-ray structure analysis at different temperatures was used to investigate the process.<sup>47</sup> These investigations have established that the ligands and eventual solvate molecules in the crystal lattice can have a

pronounced effect on the rate of intramolecular electron transfer when involved in an order–disorder type behavior upon temperature variation. It has been suggested that dynamic disorder of the former enhances the delocalization process, by providing a more symmetrical environment for the mixed-valence sites.<sup>48</sup> A crystallographic phase transition is, however, not a prerequisite for the event of valence detrapping.

The solid-state phase transition of the ethoxo-polyoxovanadium cluster **3** to the completely valence detrapped structure is accompanied by the disorder of the ethyl chains observed in the crystal structure at room temperature (Figure 6). Although a detailed crystallographic investigation of the phase transition via multi-temperature X-ray structure analysis has not been undertaken, the intervalence electron transfer is certainly linked to the motion imposed on the  $\mu$ -bridging oxygen centers by the ethyl groups' order-to-disorder transition. Thus, a fluctuation of their positions has a pronounced effect on the ligand sphere of the respective vanadium atoms, which contains four ethoxo ligands. By enabling intervalence electron transfer, the dynamic disorder is coupled to the motion of the unpaired d-electrons, as well as to the resulting motion of the remainder of the atoms involved in the process, i.e., the entire hexametallate core. This is particularly striking when comparing the thermal ellipsoids for compounds **1** and **3** at both 173 K and room temperature as shown in Figure 5; whereas the structures show comparable thermal motion at 173 K, compound **3** exhibits atomic displacement parameters at room temperature which largely exceed those of **1** at the same temperature (295 K). For sake of clarity, the disorder of the ethyl groups in the ambient-temperature structure **3**<sup>295K</sup> is not displayed in Figure 5, for which two conformational possibilities occur in the crystal structure, respectively (Figure 6).

When considering the results of the valence sum calculations, one must bear in mind that they reflect the condition of these compounds as found in the solid state at a given temperature. The valence trapping incurred is therefore specifically linked to the numerous factors encountered in this environment. Thus, packing and other effects exert a strong influence on the localization of the unpaired electrons, which would, for example, not be effective in solution. It cannot be ruled out, therefore, that the transition to a structure with disordered ethyl groups in **3**<sup>295K</sup> simply helps overcome packing effects which could be responsible for valence trapping.

**IR Spectroscopy.** In recent years, IR spectroscopy has increasingly found use in the investigation of mixed-valence compounds.<sup>34d</sup> The absorption of IR radiation occurs roughly on the time scale of a vibrational period ( $1/\nu$ ), which locates the IR method in the range of  $10^{-13}$ – $10^{-14}$  s. Thus, mixed-valence compounds with trapped valences or low rates of intervalence charge transfer show resolved absorption bands for the respective oxidation states. IR line broadening and coalescence occur if there is chemical site exchange during the lifetime of the vibrational excited state.<sup>34a</sup> Several experimental accounts

(47) (a) Wilson, C.; Iversen, B. B.; Overgaard, J.; Larsen, F. K.; Wu, G.; Pali, S. P.; Timco, G. A.; Gerbeleu, N. V. *J. Am. Chem. Soc.* **2000**, *122*, 11370–11379 and references therein. (b) Wu, C.; Hunt, S. A.; Gantzel, P. K.; Güttlich, P.; Hendrickson, D. N. *Inorg. Chem.* **1997**, *36*, 4717–4733 and references therein.

(48) Sorai, M.; Kaji, K.; Hendrickson, D. N.; Oh, S. M. *J. Am. Chem. Soc.* **1986**, *108*, 702–708.

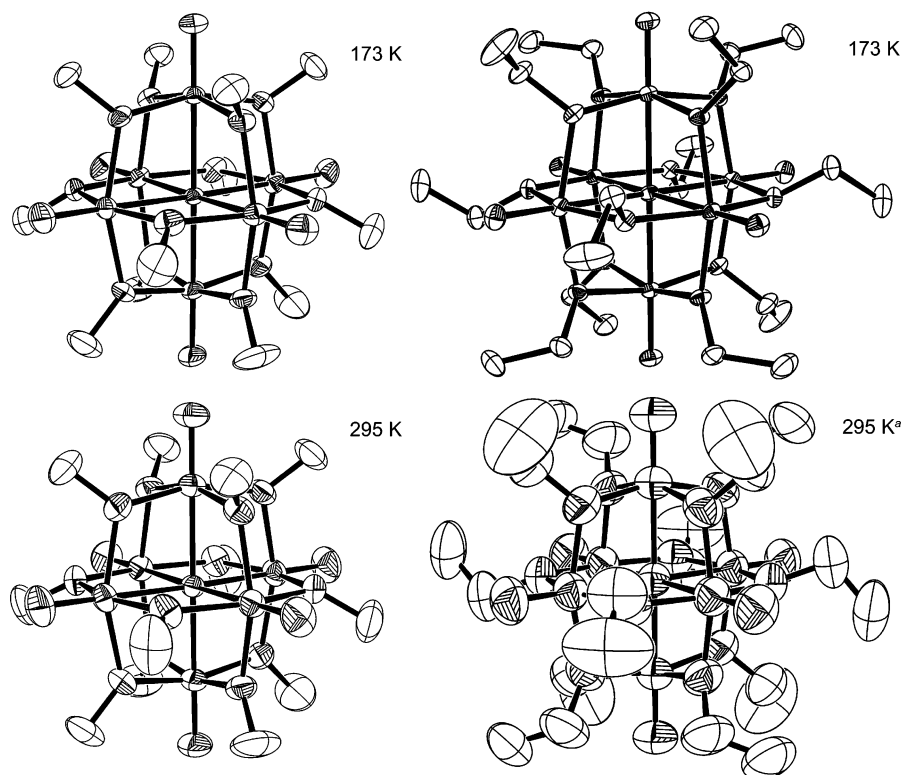


**Figure 5.** ORTEP representations of **1** (left) and **3** (right) at 173 K and room temperature respectively (ellipsoid probability: 50%). Hydrogen atoms have been omitted. The <sup>a</sup> at 295 K refers to the following: The crystallographic disorder of the ethyl groups is not shown.

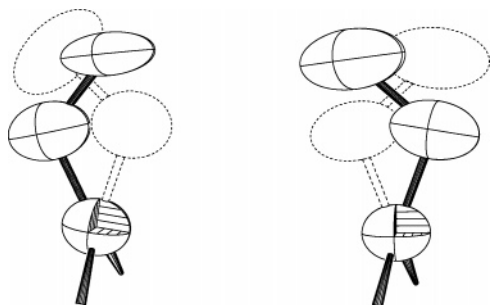


**Figure 6.** Conformational disorder of the ethyl groups in **3**<sup>295K</sup>.

of infrared line broadening and coalescence arising from dynamic coupling to electron transfer have been reported.<sup>49</sup>

Not all absorption bands in mixed-valence compounds, however, are suitable for this type of observation. Vibration modes which are strongly coupled to the electron transition, i.e., vibrations which initiate the transfer process by engendering the necessary changes in bond-lengths, are themselves involved in intervalence charge transfer. Thus, they influence the process, and as a consequence, the rate of electron transfer. In the alkoxy-polyoxovanadium clusters, this concerns all metal–oxygen stretching- and bending vibrations, particularly the V–O<sub>t</sub> stretching-, V–O<sub>b</sub>–V bending-, and V–O<sub>c</sub> stretching modes (vide supra). Correspondingly, the IR spectra of the neutral, cationic, and reduced<sup>30</sup> species all show *single* absorption bands for these vibration modes.

On the other hand, a vibration mode which is not coupled to intervalence charge transfer will also show a single absorption band. For a vibration mode to relay information on trapped

valences on the IR time scale, it must be *weakly* coupled to electron transfer and make an insignificant contribution to the electron-transfer barrier. Accordingly, the differences in equilibrium displacement for these modes between oxidation states are minor. Such modes act as “spectator” vibrations for electron transfer and provide useful oxidation-state and electron-transfer markers.<sup>34a</sup>

The O<sub>b</sub>–R stretching vibration is a good candidate for probing the mixed-valence state of the alkoxy-polyoxovanadium clusters, for while coupled to the intervalence charge transfer through the oxygen atom, the varying bond lengths caused by the vibration only has a minor impact on the rate of the electronic transition as compared to the metal–oxygen vibration modes. Although a splitting of the O<sub>b</sub>–R absorption band is not observed under the conditions employed (KBr pellet, room temperature), distinct variations in the half width of the O<sub>b</sub>–R vibration and in some cases the appearance of a shoulder were apparent. In comparison, the respective half-width and shape of the remaining features in the IR spectra of compounds **1–5** are practically constant.

Compounds **1** and **3** display relatively large O<sub>b</sub>–R stretching vibration half-widths. In addition to this, the absorption band in both compounds shows a shoulder on the low wavenumber side, which is most apparent in the IR spectrum of **1** (Figure 7). Careful study of the band shape in **1** indicates a further, weakly resolved shoulder of somewhat greater intensity on the high wavenumber side. To investigate the effect of the KBr-matrix on the band shape, both compounds were measured in solution (CH<sub>2</sub>Cl<sub>2</sub>). Here the spectra display sharper absorption bands, yet the O<sub>b</sub>–R stretching vibrations still show weakly resolved shoulders on the absorption bands’ low wavenumber side (Figure 7). Thus, according to the O<sub>b</sub>–R “spectator”

(49) Demadis, K. D.; Hartshorn, C. M.; Meyer, T. J. *Chem. Rev.* **2001**, *101*, 2655–2685 and references therein.

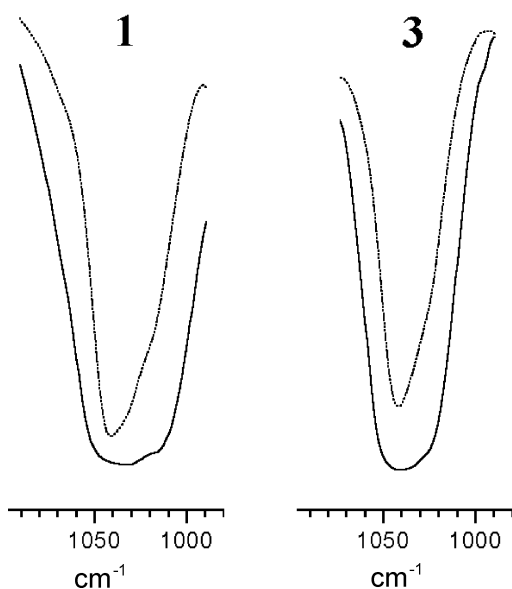


**Figure 7.**  $O_b$ -R stretching vibration in the IR spectra of **1** and **3** in KBr (—) and  $CH_2Cl_2$  (.....).

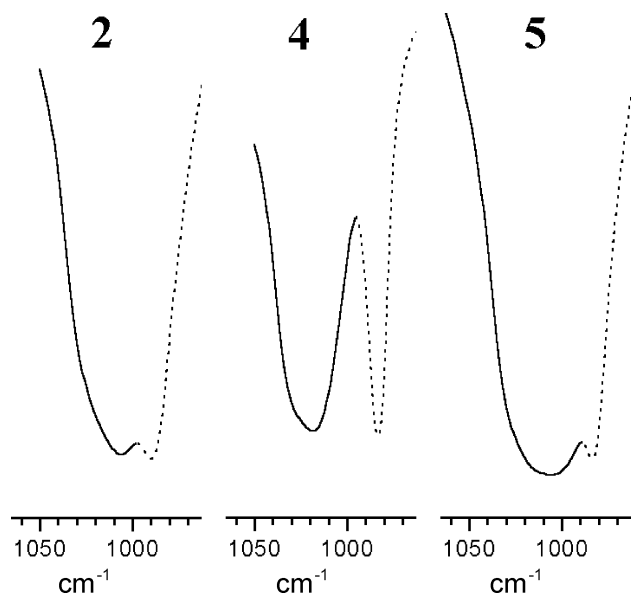


**Figure 8.**  $O_b$ -R stretching vibration in the IR spectra of **2**, **4**, and **5**. The  $V-O_t$  stretching vibration is shown as a dashed line.

vibration, the species comprising four  $V^{IV}$  centers seem to imply a certain degree of trapped valence on the IR time scale.

The IR spectra of the monocationic clusters in compounds **2** and **4** both display a narrower  $O_b$ -R stretching vibration compared to that of the neutral species (Figure 8). In the case of the methoxo cluster, the difference is distinct. Although the band presents a comparably regular shape for both compounds, a slight distortion toward the low-frequency side cannot be ignored. Finally, the dicationic ethoxo-cluster **5** shows an  $O_b$ -R absorption band which is significantly broader compared with the IR spectrum of its monocationic derivative **4**. These results suggest that the monocationic species comprising three  $V^{IV}$

centers exhibit higher intervalence charge-transfer rates than the neutral species, as well as the dicationic derivative in the ethoxo series, which contains two  $V^{IV}$  sites.

### Conclusion

The results obtained from cyclovoltammetric, IR-spectroscopic, and X-ray structural investigations clearly indicate that the methoxo- and ethoxo-polyoxovanadium cluster series  $[V^{IV}_{(4-n)}V^{V}_{(2+n)}O_7(OR)_{12}]^{n+}[SbCl_6]_n$  ( $R = -CH_3$ ,  $n = 0, 1$ ;  $R = -C_2H_5$ ,  $n = 0, 1, 2$ ) are class II mixed-valence compounds according to the Robin and Day classification scheme. Thus, valence sum calculations from X-ray structural data show that valence trapped species are found in the solid state, as well as species displaying partly and fully delocalized d-electrons, depending on the  $V^{IV}/V^V$  ratio, the nature of the  $\mu$ -bridging alkoxo ligands, as well as the collection temperature. Cyclic voltammetry indicates, based on the large splitting of the single-electron transfer redox potentials, that a high degree of electronic coupling between the metal sites in the mixed-valence species is effective, implying extensive electron delocalization in the solvated state. Finally, thanks to the existence of a so-called "spectator" vibration, IR spectroscopic results suggests that the mixed-valence clusters are partly trapped on the IR time scale, to an extent which mainly depends on the species'  $V^{IV}/V^V$  ratio. Considering these results, it can be assumed that the valence trapping ensued in the solid state is caused by cooperative effects in the crystalline phase (packing, dipole interactions, magnetic ordering, etc.).

The results presented here are by no means conclusive for the dodecamethoxo- and dodeca-ethoxo-oxo-hexa(oxovanadium) cluster series. Investigations by UV-vis and NIR spectroscopy, for example, are imperative to the further understanding of these compounds. These spectra contain, among other features, valuable information on intervalence electron transfer by means of the corresponding charge-transfer bands found therein. Aside from this, EPR spectroscopic investigations<sup>32b</sup> and magnetic measurements promise insight on the electron-transfer mechanisms (ground-state delocalization, electron hopping) and on the interplay of the unpaired d-electrons in these complex systems. Our intent is therefore to promote the presented compounds in this intensely investigated field of research as unique systems comprising a novel, highly symmetrical hexanuclear framework, in which a large number of thermodynamically stable mixed-valence states can be realized.

**Acknowledgment.** We kindly thank Mrs. Irene Brüdgam for collecting the X-ray diffraction data, and Miss Rita Friese for conducting the DSC experiments. Special thanks go to our former research students Eva-Kathrin Schillinger, Steffen Belz, Anne-Kathrin Schmidt, and Esther Fischbach for their valuable contributions to this work.

**Supporting Information Available:** Crystallographic data of compounds **1**–**5** (CIF files). This material is available free of charge via the Internet at <http://pubs.acs.org>.

JA052902B